Expansion of firn aquifers in southeast Greenland

Annika N Horlings[1], Knut Christianson[1], and Clément Miège[2]

[1]University of Washington
[2]University of Utah

November 26, 2022

Abstract

Surface melt produces more mass loss than any other process on the Greenland Ice Sheet. In some regions of Greenland with high summer surface melt and high winter snow accumulation, the warm porous firn of the percolation zone can retain liquid meltwater through the winter. These regions of water-saturated firn, which may persist for longer than one year, are known as firn aquifers, commonly referred to as perennial firn aquifers. Here, we use airborne ice-penetrating radar data from the Center for Remote Sensing of Ice Sheets (CReSIS) to document the extent of four firn aquifers in the Helheim, Ikertivaq, and Køge Bugt glacier basins with more than six repeat radar flight lines from 1993 to 2018. All four firn aquifers first appear and/or show decadal-scale inland expansion during this time period. Through an idealized energy-balance calculation utilizing reanalysis data from Modèle Atmosphérique Régionale (MAR) regional climate model, we find that these aquifer expansions are driven by decreasing cold content in the firn since the late 1990s and recently increasing high-melt years, which has reduced the firn's ability for refreezing local meltwater. High-melt years are projected to increase on the Greenland Ice Sheet and may contribute to the continued inland expansion of firn aquifers, impacting the ice sheet's surface mass balance and hydrological controls on ice dynamics.

Posted on 26 Nov 2022 — CC-BY 4.0 — https://doi.org/10.1002/essoar.10511604.1 — This a preprint and has not been peer reviewed. Data may be preliminary.

Expansion of firn aquifers in southeast Greenland

Annika N. Horlings[1], Knut Christianson[1], Clément Miège[2]

[1]Department of Earth and Space Sciences, University of Washington, Seattle, WA, USA
[2]Department of Geography, University of Utah, Salt Lake City, Utah, USA

Key Points:

- We generate a time series of four perennial firn aquifers in southeast Greenland from 1993 to 2018 using ice-penetrating radar data.
- The four firn aquifers first appear and subsequently expand upstream toward the ice-sheet interior during the time period.
- Firn-aquifer expansion is correlated with decreasing firn cold content and recent high-melt years.

Corresponding author: Annika N. Horlings, annikah2@uw.edu

Abstract

Surface melt produces more mass loss than any other process on the Greenland Ice Sheet. In some regions of Greenland with high summer surface melt and high winter snow accumulation, the warm porous firn of the percolation zone can retain liquid meltwater through the winter. These regions of water-saturated firn, which may persist for longer than one year, are known as firn aquifers, commonly referred to as perennial firn aquifers. Here, we use airborne ice-penetrating radar data from the Center for Remote Sensing of Ice Sheets (CReSIS) to document the extent of four firn aquifers in the Helheim, Ikertivaq, and Køge Bugt glacier basins with more than six repeat radar flight lines from 1993 to 2018. All four firn aquifers first appear and/or show decadal-scale inland expansion during this time period. Through an idealized energy-balance calculation utilizing reanalysis data from Modèle Atmosphérique Régionale (MAR) regional climate model, we find that these aquifer expansions are driven by decreasing cold content in the firn since the late 1990s and recently increasing high-melt years, which has reduced the firn's ability for refreezing local meltwater. High-melt years are projected to increase on the Greenland Ice Sheet and may contribute to the continued inland expansion of firn aquifers, impacting the ice sheet's surface mass balance and hydrological controls on ice dynamics.

1 Plain Language Summary

Warm atmospheric temperatures over the Greenland Ice Sheet can melt snow at the surface, producing liquid meltwater that can infiltrate downward into denser and older snow known as firn. The firn can retain this liquid meltwater continuously for more than one year in certain regions of the ice sheet that have high snow accumulation and high surface melt. These water-saturated regions of firn are called firn aquifers, which are important in understanding the ice sheet's mass loss to the oceans. To determine the evolution of firn aquifers in Greenland and what factors primarily influence their behavior, we examine airborne ice-penetrating radar data that were collected from 1993 to 2018. From the repeat detections of four firn aquifers in southeast Greenland, we find that the aquifers first appear and/or expand inland during this time period. Regional historical climate data and an idealized energy budget calculation suggest that aquifer expansions are driven by warming firn since the 1990s: the firn is not cold enough to refreeze increasingly large amounts of surface melt, and therefore the meltwater remains in a liquid state. More extreme warm summers are expected for Greenland, which may contribute to the formation and continued expansion of firn aquifers.

2 Introduction

Currently, the Greenland Ice Sheet is the single largest cryospheric contributor to sea-level rise and, in recent decades, has lost mass at an increasing rate (Mouginot et al., 2019; Van den Broeke et al., 2016; Shepherd et al., 2020). Of the Greenland Ice Sheet's mass loss since 2000, surface melt constitutes approximately 55% (Shepherd et al., 2020). However, processes involved in meltwater transit through the supraglacial, englacial, and subglacial hydrological systems of the ice sheet are not well understood, especially within the context of a warming climate. In some regions of the ice sheet with high summer surface melt combined with high winter snow accumulation, the warm porous firn of the percolation zone can retain surface meltwater without refreezing during winter; these water-saturated regions of firn are known as firn aquifers (Forster et al., 2014). Firn aquifers can influence ice-sheet flow and surface mass balance (Poinar et al., 2017, 2019; Montgomery et al., 2020), yet remain a relatively understudied piece of the ice sheet's hydrological system.

In this study, we focus on firn aquifers which retain liquid meltwater for more than one year (commonly known as perennial firn aquifers; we shorten this terminology to firn aquifer). While recent studies found that firn aquifers do not contribute to long-term water storage that could substantially buffer sea level (Miller et al., 2020), quantifying the evolution of firn aquifers in the present and future is important because they affect ice-sheet dynamics and thermodynamics by: (1) changing the seasonal behavior of the hydrologic system, through creation of englacial and subglacial channels that persist over the winter (Poinar et al., 2017); (2) influencing firn-compaction processes, meltwater flow and meltwater retention in the firn (Munneke et al., 2014, 2015; Miller et al., 2020); (3) impacting the thermal regime of the ice sheet, as they represent large reservoirs of latent heat (Munneke et al., 2015); and (4) contributing to structural loading of ice shelves, especially on the Antarctic Peninsula, which may enhance hydrofracturing and lead to their eventual breakup (Montgomery et al., 2020).

The first well-studied seasonal firn aquifers were documented beginning in the 1980s in the high-accumulation and high-melt regions of temperate alpine glaciers; for example, the late summer/early autumn aquifers of the Oetztal Alps in Austria, Storglaciären in Sweden, and South Cascade Glacier in the United States (Oerter & Rauert, 1982; Fountain, 1989; Fountain & Walder, 1998; Schneider, 1999; Jansson et al., 2003). During the Arctic Circle Traverse expedition in 2011, firn aquifers were first observed in southeast Greenland from firn cores (Forster et al., 2014). Subsequently, several field studies conducted extensive in-situ and geophysical measurements at a firn aquifer located in upstream Helheim Glacier in southeast Greenland (summarized in Miller et al. (2020)). Recent studies have also assessed firn aquifers there and elsewhere, including along the perimeter of the Greenland Ice Sheet, on the Holtedahlfonna Ice Field in Svalbard, in the St. Elias Mountains of Canada and Alaska, and on the Wilkins Ice Shelf in Antarctica, and have focused on characterizing aquifer extent, monitoring aquifer changes, and understanding the physical principles guiding aquifer formation and behavior (Forster et al., 2014; Koenig et al., 2014; Christianson et al., 2015; Miège et al., 2016; Chu et al., 2018; Miller et al., 2020; Montgomery et al., 2020; Humphrey et al., 2021; Ochwat et al., 2021).

Despite this, little is known about how changes in atmospheric forcing influence firn-aquifer extent, water flow, timescale of formation, evolution, and the role of firn aquifers in ice-sheet hydrology (Miller et al., 2021), motivating further study. It is generally accepted that the formation of firn aquifers requires high summer surface melt (approximately >0.24-0.65 m yr^{-1} w.e.) and high snow accumulation (approximately >0.8 m w.e. yr^{-1}) (Forster et al., 2014; Miller et al., 2020). These conditions are pervasive especially in the percolation zone of the southeastern periphery of the Greenland Ice Sheet. There, firn aquifers may occupy roughly 54,800 km^2, as estimated through Sentinel-1 radar data (Brangers et al., 2020).

For the southeast Greenland Ice Sheet, Miége et al. (2016) documented the widespread existence of firn aquifers using ice-penetrating radar data and showed that the firn aquifer detected at Helheim Glacier expanded toward the ice-sheet interior from 2010 to 2014. Miller et al. (2020) highlighted continued expansion of the Helheim firn aquifer until 2017. Firn aquifers have likely existed undetected for over 40 years in the deep firn of the Greenland Ice Sheet's percolation zone, as suggested by the congruence of recent mapped extent of firn aquifers (Forster et al., 2014) and observations from historical 1978 Ku-band radar backscatter imagery (Miller et al., 2020). Longer and more continuous time-series analysis of firn aquifers using ice-penetrating radar data (the most direct remote-sensing method of imaging firn aquifers) has, however, not yet been conducted. In addition, the recent expansion of the Helheim firn aquifer (Miège et al., 2016; Miller et al., 2020) has been informally hypothesized to result from increased surface melt as locations transition to temperate from warmer atmospheric temperatures (Miller et al., 2020). While aquifer recharge has been observed in response to high melt (Christianson et al., 2015), the link between changes in atmospheric forcing, especially more frequent and more intense melt seasons, and multi-decadal aquifer response has not been thoroughly investigated. Modeling studies (Vandecrux et al., 2020; Ochwat et al., 2021) have begun to

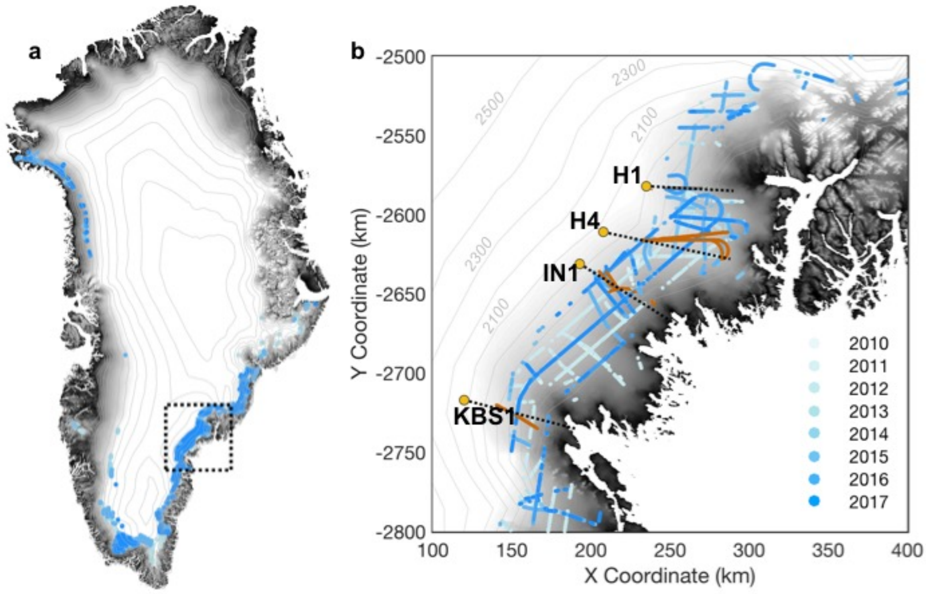

Figure 1. a) Map of southeast Greenland showing aquifer detections from Miège et al. (2016). The dashed box shows our focus region. b) The four firn-aquifer sites that are the focus of this study, as shown in reference to the aquifer detections from Miège et al. (2016). The aquifer sites are labeled: Helheim 1 (H1), Helheim 4 (H4), Ikertivaq N1 (IN1), and Køge Bugt S1 (KBS1). Dashed lines show the location of the reference coordinates on which our aquifer detections along the four repeat flight line segments (brown) were projected onto, roughly in the direction of the surface-elevation gradient. Elevation contours (relative to the WGS84 Ellipsoid) are derived from MEaSUREs Greenland Ice Mapping Project (GIMP) Digital Elevation Model, Version 1, gridded to a polar stereographic projection (EPSG:3413).

evaluate this problem; however, there remains substantial disagreement among firn meltwater models, especially at firn-aquifer sites (Vandecrux et al., 2020).

We motivate our study through the following questions: Has the spatial extent of firn aquifers across southeast Greenland changed in recent decades? Are years with high meltwater production impacting the expansion of these firn aquifers? We hypothesize that upstream expansion of firn aquifers (toward the ice-sheet interior) in southeast Greenland will occur in response to high-melt years if the firn has enough heat to inhibit refreezing. Alternatively, firn aquifers may intermittently drain into downstream crevasses and/or the aquifer water table may decrease in depth, hindering expansion. We use a subset of mapped firn aquifers to test our hypothesis: four locations in southeast Greenland with more than six usable repeat radar flight lines. We extend the firn aquifer time series to as far back as 1993 by identifying the presence of the aquifers in airborne ice-penetrating radar data.

Our study is the first to extend the firn aquifer time series to earlier than 2010. It is also the first to consider regions beyond Helheim Glacier to evaluate trends in expansion of firn aquifers on regional scales across southeast Greenland. Finally, it is the first to use regional climate reanalysis data to evaluate climate controls on the expansion of firn aquifers in Greenland.

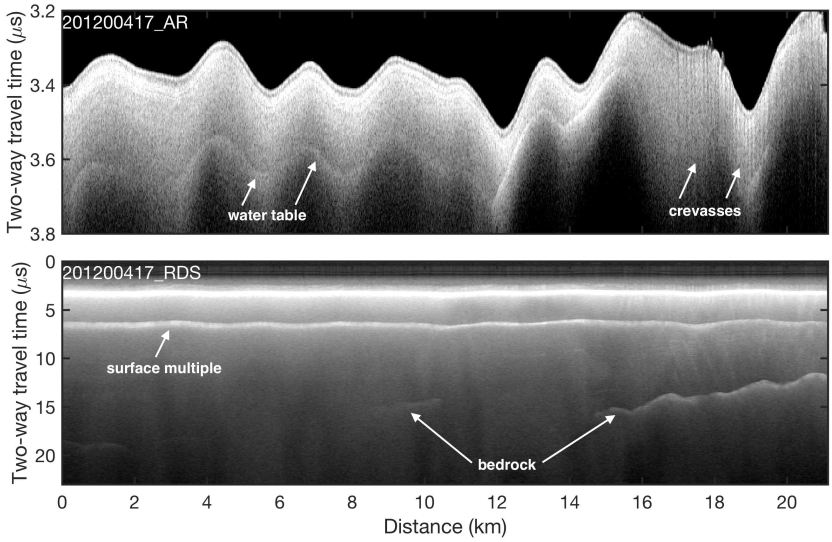

Figure 2. a) Accumulation radar (AR) and b) MCoRDS (RDS) profiles showing the firn aquifer at upper Helheim Glacier (H1 in Figure 1), which were collected on April 17, 2012. The firn water table is the bright continuous reflector in the upper firn in the AR profiles. The absence of the bed reflector in the RDS data correlates with the presence of the water table reflector in the accumulation radar profile. Left-hand side of the figure is toward the ice-sheet interior.

3 Materials and Methods

3.1 Sites

We assess four firn aquifers in southeast Greenland (Figure 1). H1 is located in upper Helheim Glacier, between 1450 m and 1800 m elevation; IN1 is located in upper Ikertivaq Glacier between 1300 and 1750 m elevation; H4 is located south of H1 and north of IN1, between 1400 and 1800 m elevation; and KBS1 is located inland of Køge Bay, and lies between 1300 and 1700 m elevation. We focus on these sites because have multiple repeat CReSIS flight lines exceeding six individual years that also trend roughly interior-seaward (i.e., along the surface-elevation gradient of the ice sheet).

3.2 CReSIS Airborne Radar Sounding Observations

We use data from two airborne ice-penetrating radar systems designed and operated by the Center for the Remote Sensing of Ice Sheets (CReSIS) at the University of Kansas: the accumulation radar (AR) and the CReSIS Multichannel Coherent Radar Depth Sounder (RDS) systems (Rodriguez-Morales et al., 2013; Leuschen et al., 2014). Both the AR and RDS radar systems operated aboard NASA's Operation IceBridge (OIB) aerogeophysical surveying campaigns aboard P-3 aircraft (2010 - 2019). The RDS system was also operated on a C-130 Hercules aircraft in 2015; however, the AR system was omitted due to non-optimal wing configuration for mounting antennas. Additionally, the AR system was operated in 2019 on a Twin Otter (TO) aircraft. Earlier version of the RDS system were operated by the Radar Systems and Remote Sensing Laboratory at the University of Kansas on earlier aerogeophysical missions dating back to 1993 aboard P-3, DC8, C-130, TO, and Basler (DC3) aircraft.

The AR system is an ultra-high-frequency radar operated with center a frequency of 750 MHz and bandwidth of 300 MHz. It images the upper portion of the ice sheet, penetrating up to 500 m in depth for smooth, spectral targets (Leuschen et al., 2014; Miège et al., 2016). AR radar profiles are generally available Greenland-wide from 2010 - 2014 and 2017 - 2019. The AR system directly images the water table of a firn aquifer as a high-amplitude reflector, due to the high dielectric contrast between dry and water-saturated firn (Miège et al., 2016; Chu et al., 2018).

The RDS system operated at many different center frequencies over time during different surveys, but always at a lower frequency than the AR system, which allows imaging to the ice-sheet bed. RDS data are available Greenland-wide from 1993, 1995 - 1999, and 2001- 2019. We use a novel technique to determine the presence of a firn aquifer, first pioneered by Miége et al. (2016): within the RDS radar profiles, the firn aquifer can be identified via its interference with subsequent reflections. The disappearance of the reflection from the ice-sheet bed (and disappearance of internal layers) indicates the presence of water, as water within the firn increases the attenuation and scattering of the radar wave. Comparison of the AR and RDS datasets during overlapping years corroborates this interpretation (Figure 2; Supporting Information).

3.3 Radar Interpretation

We use ImpDAR, an open-source radar processing and interpretation toolbox (Lilien et al., 2020), to interpret radar signals and map the firn aquifers from the CReSIS radar sounding data. ImpDAR is used to digitize the bright firn water-table reflector in the AR radar profiles and to map the inferred extent of a firn aquifer by the absence of internal layers and bed reflector in the RDS radar profiles, as suggested in Miége et al. (2016). We categorize extent as the interior-seaward linear distance spanned by the aquifer along chosen flight lines. We project extents from flight lines that are oblique to the coast onto an interior-seaward direction.

Agreement between AR and RDS firn-aquifer detections for each basin is high (Figure 2; Supporting Information), where the bright reflector in the AR radar profiles of the water table (illustrating water-saturated firn) correlates with the disappearance of the bed reflector in contemporaneous RDS radar profiles at the same location. Miége et al. (2016) also noticed good agreement when identifying the firn-aquifer locations on the two airborne radar systems. Additionally, water-volume data from magnetic resonance soundings (Legchenko et al., 2018) has shown good agreement between high water volumes at a firn-aquifer site and disappearance of the bed reflector in the RDS data (Supporting Information). These results allow us to confidently extend the time series of firn-aquifer extent to the start of the RDS observations in 1993, when only RDS data are available. Because picking the aquifer extent in the radar profiles was not a fully automated process and is subject to human bias, there is some uncertainty in the identified aquifer extent. These uncertainties are described further in Miége et al. (2016). Disagreement in aquifer detections between the two radar systems occurs primarily where the intensity of internal reflectors weaken at the edges of the water table or at the edges of the disappearing bed reflector.

We define aquifer "expansion" as the progression of aquifer detections toward the ice-sheet interior as determined by changes in linear extent. In contrast, we use the concept of aquifer "migration" as the progression of both upper and lower linear extent of the aquifer toward the ice-sheet interior. Also, we define a single "firn aquifer" as a near-continuous detection (no detection gaps >5 km) of the water table and/or associated disappearance of the bed along the chosen repeat flight lines. We acknowledge that the aquifers that we identify may be interconnected in a larger aquifer system; however, with the limited flight extent, we cannot verify that they are connected and therefore assume that the identified aquifers in this study operate largely independently from each other.

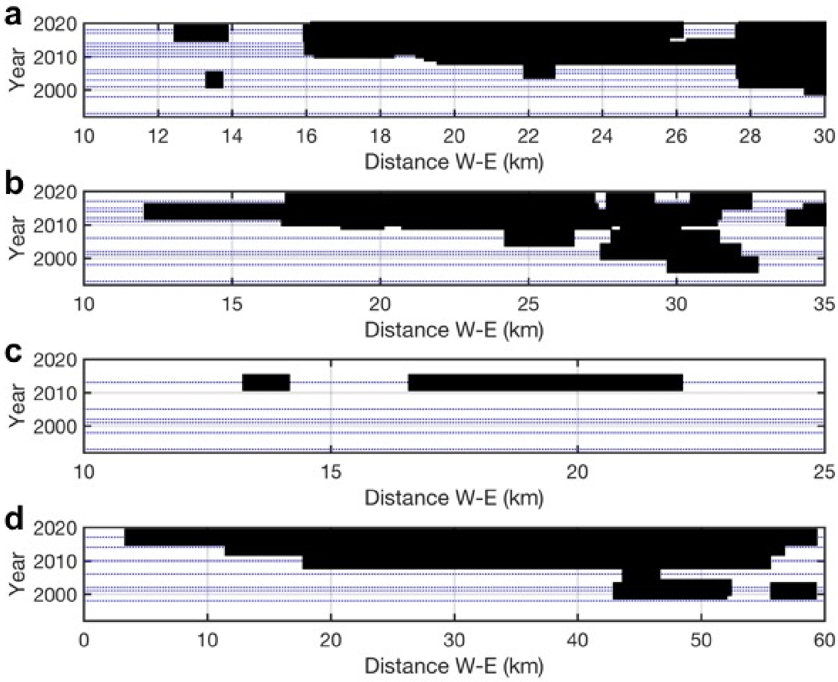

Figure 3. a) Firn-aquifer detections along each repeat flight line using both the AR and RDS radar profiles: a) H1, b) IN1, c) KBS1, and d) H4. Blue dotted lines indicate years that data is present. The small detection upstream in 2003 at H1 is real. We assume that each aquifer incorporates the detections along the repeated flight line as long as there are no gaps greater than 5 km.

3.4 Regional Climate Model

To assess the climatic factors contributing to aquifer evolution, we use reanalysis data from the Modèle Atmosphérique Régional MAR 3.5.2 (Fettweis & Rennermalm, 2020), a regional atmospheric model designed to simulate kilometer-scale to continental-scale processes over multi-decadal timescales in the polar regions. Firn-aquifer formation is governed by the balance of generated surface meltwater infiltrating downward into the firn and the ability of the firn to refreeze this meltwater. We therefore analyze the annual melt, snow accumulation, the melt-to-surface-mass-balance ratio, wintertime (January-March) temperature, number of days above a defined melt threshold (0.5 mm per day), and annual rainfall. We take the mean of these climate parameters for the closest cell to the aquifer locations because MAR's resolution is relatively coarse (20 km) for application to a single aquifer. In addition, we determine the long-term trend, decadal mean and standard deviation, and the change points of the time series for each climate parameter, defined as the time instant at which the mean of the time series changes abruptly, through a parametric global method (Lavielle, 2005; Killick et al., 2012) (Supporting Information).

4 Results

4.1 Multidecadal Airborne Radar Sounding Observations

We present evidence of multidecadal firn-aquifer expansion from ice-penetrating radar profiles in southeast Greenland from 1993-2018. All four repeat flight lines show a first detection of the firn aquifers between 1993 and 2002 and then subsequent expansion toward the ice-sheet interior (Figure 3). Outside of these areas, other repeat flight lines in southeast Greenland are unclear as to whether expansion of other aquifers occurs, likely because of the existence of few repeat flight lines. We describe each site in further detail.

4.1.1 Helheim Firn Aquifer (H1)

The most repeat flight-line coverage is over H1 with a combination of RDS and AR data available in 1993, 1998, 2001, 2003, 2005, 2006, 2008, 2010-2014 and 2016-2018. Both AR and RDS radar imagery individually and collectively show the expansion upstream toward the ice-sheet interior (Figure 3). The aquifer is first detected in 1998; it subsequently expanded 0.3 km from 1998-2001; 1.8 km from 2001-2003; did not expand from 2003-2005; and expanded 0.1 km between 2005 and 2006. Following this, a substantial expansion occurred between 2006 and 2010, where the firn aquifer expanded upstream by 8.1 km inland. This was followed by a further 3-km expansion until 2012. An upstream, more isolated extension of the aquifer (3.6 km upstream) appears to persist in 2017 and disappears in 2018, while the upstream extent of the main aquifer appears to remain approximately similar from 2012-2018 (Figure 3).

Increases in the depth of the water table (i.e., water discharge) in 2012 have been hypothesized as a drainage event through downstream crevasses (Miège et al., 2016; Miller et al., 2020). This drainage may have a delayed effect on suppressing inland expansion, as the inland portion of the water table is slower to respond to the drainage compared to the downstream end nearest to the crevasses. Observations show recharge (decrease of water-table depth) from 2013-2016, which is associated with progressive expansion.

4.1.2 Ikertivaq North Firn Aquifer (IN1)

Both RDS and AR data available for IN1 is 1993, 1998, 2001, 2002, 2006, 2011, 2012, 2014, 2015, and 2017. The first detection of the aquifer at IN1 is in 1998. From 1998 to 2001, the aquifer slightly decreased in upstream extent by 0.6 km. From 2001 to 2002, the aquifer expanded upstream 2.9 km and subsequently expanded 3.2 km upstream from 2002 to 2006. From 2006 to 2011, the aquifer expanded 5.5 km upstream; from 2011-2012, it expanded 2 km; and between 2012-2014, the aquifer expanded 4.7 km, and finally decreased in upstream extent from 2014 to 2017 by 4.8 km.

4.1.3 Koge Bugt South Firn Aquifer (KBS1)

RDS data are available for KGBS1 for 1993, 1998, 2001, 2002, 2005, and 2013. The main aquifer is first detected in 2013; however, we do not have any subsequent data along the repeat flight line, so cannot present any results on further its evolution.

4.1.4 Helheim 4 Firn Aquifer (H4)

RDS data are available for H4 in 1993, 1998, 2001, 2002, 2006, 2008, 2010, 2014, 2015, 2017, and 2018. The first detection of H4 was in 2001. While the aquifer decreased in upstream extent by 1.2 km from 2001 and 2002, the aquifer subsequently expanded by 0.5 km from 2002 to 2006. Then, between 2006 and 2010, the aquifer expanded by

25.9 km upstream; between 2010 and 2014, the aquifer expanded by 6.3 km; and between 2017 and 2018, the aquifer expanded by 8.1 km upstream.

Altogether, our analysis of repeat ice-penetrating radar profiles for four aquifers suggests that firn aquifers in Southeast Greenland are expanding upstream toward the ice-sheet interior and to higher elevations. However, we do not observe that the lower extents of the firn aquifers are migrating toward the ice-sheet interior.

4.2 Climate Forcing on Firn Aquifers in Southeast Greenland

Cumulative annual melt generally increases from 1948 to 2017, though the trend is not statistically significant ($R^2 = 0.338$). Cumulative annual melt exceeding one standard deviation from the long-term mean occurs during the years 1957, 2004, 2005, 2007, 2010, 2012, 2014, and 2016. The most substantial high-melt year over the aquifer sites was in 2012, which is also known to be a significant melt year Greenland-wide (Nghiem et al., 2012). Winter snow accumulation is highly variable and does not show a significant trend over this time period. The melt-to-surface mass balance ratio is dominated by the annual melt signal. Annual winter surface temperatures show a slight long-term warming trend, but this is not statistically significant. Extreme annual rainfall occurred in some years such as 2010. The number of days above the defined melt threshold ($>$ 0.5 mm per year) increases slightly beginning in the mid 1990s. However, for high-melt years such as 2007 and 2012, the number of days occurring above this melt threshold are within one standard deviation of the long-term mean despite high total annual melt. This suggests that a few very intense melt events dominated those melt seasons. This is in line with satellite observations that show the 2012 melt season was governed by intense short-lived melt events (Nghiem et al., 2012).

Of the climate parameters analyzed from 1948 to 2016, we find most substantial recent changes in the surface melt and winter temperature (Figure 4). We calculated decadal averages and determined change points, which determine the time at which the mean of the time series changes abruptly. These analyses show that the surface melt increase is most marked from approximately 2004 and the winter temperature increased substantially after 2009. All other analysis of melt, snowfall, temperature, and rainfall parameters from MAR for 1948-2016 are presented in the Supporting Information.

4.3 Linking Aquifer Expansion to Climate through Firn Cold Content

To link the firn-aquifer observed expansion to changes in climate, we investigate the energy balance that permits aquifer formation. Following (Culberg et al., 2021) and (Humphrey et al., 2021), we relate the cold content (CC) of the firn with the latent heat content from surface melt (LH) from 1948 to 2017. While firn models can calculate cold content, meltwater schemes and their ability to form aquifers are not consistent across models (Vandecrux et al., 2020). Therefore, we use idealized calculations to estimate this complex thermodynamic system. We define the cold content and latent heat for the upper 20 m of the firn column as:

$$CC = 20c\rho_f T_f. \tag{1}$$

$$LH = L_h M \rho_w. \tag{2}$$

Here, c is the heat capacity of ice, ρ_f is the volume-weighted mean annual density of the firn, T_f is the absolute value of the mass-weighted mean annual firn temperature in degrees Celsius, L_h is the latent heat of fusion for water, M is the total annual melt in m w.e.q., and ρ_w is the density of water. We can then quantify the capacity of the upper firn column to refreeze surface meltwater as the ratio between latent heat and cold

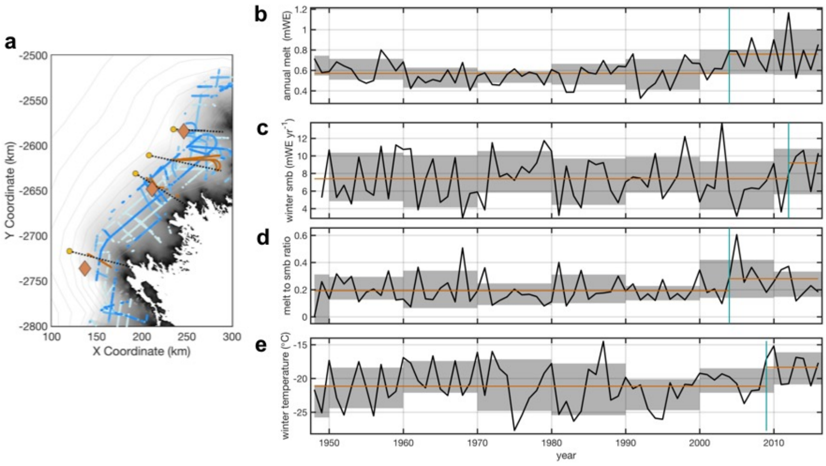

Figure 4. MAR reanlysis for the upstream portion of the aquifers. We choose to show these variables because firn-aquifer formation is governed by the balance of generated surface meltwater infiltrating downward into the firn and the ability of the firn to refreeze this meltwater. (a) Map showing aquifer detections from Miège et al. (2016) (blue) and from this study (brown). MAR cells closest to the aquifer sites (brown diamonds) have a resolution of 20 m. (b) Total annual melt. (c) Previous winter's surface mass balance. (d) Ratio of melt and the previous winter's surface mass balance. (e) Mean winter temperature. Decadal mean with decadal standard deviation is represented in gray. Blue vertical lines denote the change point for the time series mean. Brown horizontal lines denote the mean for the time period before and after the detected change point. Location of MAR cell extent nearest to the aquifers over which the climate output was averaged shown in map.

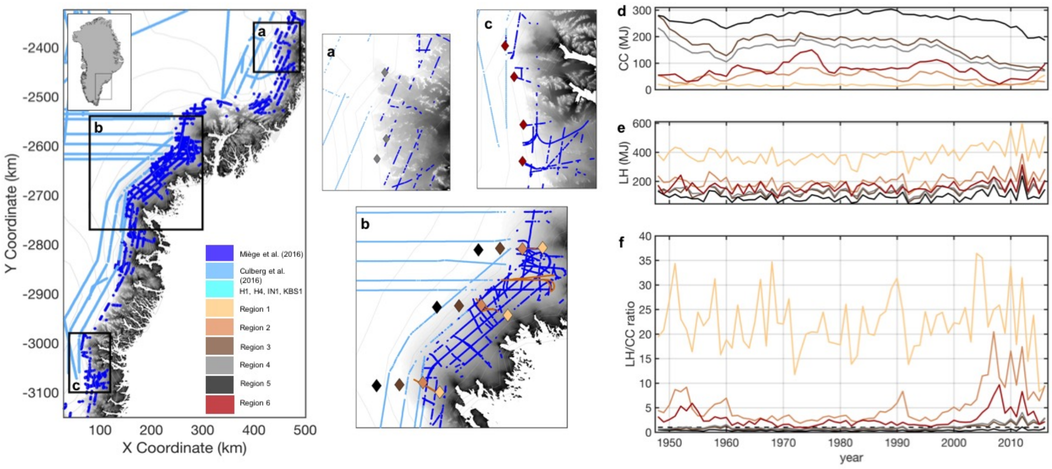

Figure 5. (a-c) Maps showing the subset of regions over which the MAR output was averaged. Diamonds denote the query locations corresponding to each region 1-6. Aquifer detections from Miege et al. (2016) in royal blue are shown. The ice layers from Culberg et al. (2016) in light blue are inland and adjacent to the aquifers. Aquifer detections from this study are shown in brown. (d) Cold content averaged over each region, colors corresponding locations of cells shown on the map. (e) Latent heat content from meltwater. (f) The ratio of latent heat to cold content.

content (R). When R becomes large, the firn loses its ability to refreeze meltwater and when R becomes small, the firn has sufficient cold content for refreezing. Therefore, the energy balance permitting aquifer formation (R>1) is:

$$L_h M \rho_w > 20 c \rho_f T_f. \tag{3}$$

Based on this equation, we define the potential for aquifer formation as warm firn conditions with a plentiful meltwater supply. These conditions are necessary but may be insufficient for firn-aquifer formation, as surface topography and crevasse proximity also influence location and evolution of aquifers.

We calculate the cold content, latent heat, and ratio (R) at six different sites in southeast Greenland representing different regions (Figure 5). We delineate these six regions to generally exemplify the state of the firn at and adjacent to the firn-aquifer sites that are a focus of this study (regions 1-4) and at higher and lower latitude sites at the upstream extent of other detected aquifers (regions 5-6, respectively). For each of these general regions, we take the climate conditions described by the MAR cell that is closest to: (1) low-elevation aquifer sites, at the downstream edges of the aquifers of this study; (2) upstream aquifer sites, at the most upstream edges of the aquifers of this study; (3) site adjacent to the upstream aquifer edge and the ice-layer region, where the aquifers are expanding into; (4) interior site, inland and at higher elevations to the aquifers of this study and within the ice-layer region; (5) higher-latitude upstream aquifer sites, at the most upstream edges of detected aquifers in eastern Greenland; and (6) lower-latitude upstream aquifer sites, at the most upstream edges of detected aquifers in southern Greenland.

Our calculations show that the firn cold content is decreasing at and to the interior of the upstream edges of the aquifers of this study (2, 3 and 4) starting in the late 1990s and early 2000s, as well as other aquifers farther north (5) and south in latitude (6). The latent heat to cold content ratios (R) at the northern-latitude sites (6) and adjacent to the upstream edge of the aquifers of this study (3) increase to greater than one during this time. R at the interior site (4) generally remains less than one, though reached this value in 2012. The firn cold content at the higher-elevation sites directly upstream of the four aquifers (3 and 4) have higher cold content than within the aquifer sites (1 and 2). The latent heat to cold content ratios are lowest of all sites at the most inland site (4), down to 0.5. The lowest-elevation site at the downstream portion of the aquifers (1) shows the lowest cold content that does not show a trend, and also has the highest latent heat to cold content ratio, which also appears to show no trend.

5 Discussion

Our observations show that the four firn aquifers that we assessed through ice-penetrating radar are expanding toward the ice-sheet interior and to higher elevations non-monotonically. We also observe substantial interannual variability in aquifer extent that may be due to abrupt drainages or changes in local meltwater availability.

The generally accepted paradigm is that firn-aquifer formation occurs under high-melt conditions, which allow surface meltwater to infiltrate deep within the firn, and under high-accumulation conditions, which insulate the liquid meltwater from the winter cold (Munneke et al., 2014). Liquid meltwater exists within the firn when top-down refreezing (from the winter cold) and lower-boundary refreezing (from the cold deep firn, as a result of loss of heat from diffusion ahead of the infiltrating water front) are unable to refreeze the infiltrating meltwater (Humphrey et al., 2021). The energy balance permitting aquifer formation can be generally summarized by Equation 3, which states that the downward infiltration of water will be halted if the cold content of the firn is greater than the latent heat of the infiltrating meltwater. While diffusion ahead of the water front can be theoretically large and prevent meltwater from accessing the full firn pore space, aquifers at locations with high meltwater availability will more likely be influenced by top-down refreezing (Humphrey et al., 2021). The idealized energy balance of firn in high-melt regions illustrated in Equation 3 shows that the link between firn-aquifer formation and atmospheric forcing is mainly through the snow melt (supply of liquid water and latent heat), the snow accumulation (for the pore space and buffer from winter temperatures), and surface-air temperature (which controls the cold content of the firn).

Our observations indicate a decrease in the firn's capacity for refreezing meltwater in southeastern Greenland beginning in the late 1990s and early 2000s. Specifically, the firn cold content adjacent to the upstream edge of H1, IN1, KBS1, and H4 aquifers (regions 2 and 3) consistently lost the capacity to refreeze the increasing volume of meltwater beginning in 1997. We observe the lowest cold content and highest R value attained in 2007, 2010, and 2012, which correspond to notable high-melt years. Our radar detections of the firn aquifers show formation during the late 1990s, followed by a non-monotonic expansion that continues until the most recent detections in 2018 (excluding KGBS1, where the last usable radar profile is in 2013). While drainages and connections to other aquifers may add complexity, which can be difficult to assess with existing radar profiles, our results suggest that the firn aquifers in southeast Greenland are expanding inland in response to the firn's decreased capacity for refreezing and an increase in surface meltwater availability. This confirms our hypothesis: that upstream expansion of firn aquifers in southeast Greenland will occur in response to high-melt years if the firn is warm enough to inhibit refreezing. Recent coupled firn-thermodynamic and hydrology modeling of meltwater infiltration at DYE-2 show that the firn is strongly impacted by high-melt years such as those in 2012 and 2019 through the increase of firn temperature, ice content, and firn density, which subsequently reduces the firn's ability to retain meltwater (Samimi et al., 2021), which supports our results.

Ice layers, which occur when percolating meltwater is refrozen following high-melt years, occur directly upstream of firn-aquifer locations on the ice sheet (Figure 5) (Culberg et al., 2021). The change in the energy balance at higher elevations above the firn aquifers is reflected in our calculations of the ratio of cold content and latent heat from meltwater. This switch in firn characteristics is important to understand because the presence of extensive ice layers complicates water percolation (Miège et al., 2016). Ice layers can isolate deep firn pore space to force meltwater to discharge into efficient surface runoff systems ("firn runoff regime"; (Machguth et al., 2016)), or to create perched water tables (Christianson et al., 2015; Miège et al., 2016). While we do not observe any melt layers in the ice-penetrating radar datasets for the chosen flight-line segments, it is suspected that melt-layer formation may promote firn-aquifer expansion by "priming" the firn through the release of latent heat into the surrounding cold firn during refreezing or by amplifying meltwater input downstream through migration of the meltwater laterally along the low-permeability ice layers under low hydraulic gradients (Miège et al., 2016; Culberg et al., 2021). Thus, melt layers may introduce an additional local hydrological process that influences aquifer formation and behavior. For example, the intense melt year in 2012 initiated ice-layer formation upstream of the firn aquifer at Helheim Glacier, which may have formed a perched firn aquifer and increased meltwater input into the aquifer region (Miège et al., 2016; Culberg et al., 2021).

We also observe that there are multiple timescales of firn-aquifer behavior. Decadal-scale aquifer behavior is driven by a decrease in cold content, increase in atmospheric warming, and increase in frequency of high-melt years. In contrast, lower amplitude interannual variability may be controlled by aquifer drainages, while seasonal expansion and retreat of the aquifer is due to fluctuating meltwater availability through the year. While there is temporal variability between firn aquifers, our results suggest that warming firn conditions generally facilitate inland expansion in tandem with increasingly high meltwater availability. Ultimately, upstream and inland migration of glaciological facies (e.g., superimposed-ice zone, wet-snow zone, and the percolation zone), as seen in similar climate regimes to the Greenland Ice Sheet, such as the Devon Ice Cap (Gascon et al., 2013), will likely influence future firn-aquifer and ice-layer formation on the Greenland Ice Sheet; however, we did not detect the migration of the lower limit of firn aquifers.

With the likely increase in the frequency and duration of high summer surface melt due to warming conditions over Greenland Ice Sheet during the 21st century (Field et al., 2012), firn aquifers likely will expand and affect ice-sheet hydrology and mass balance over larger areas. For example, firn-aquifer water can maintain small englacial channels through the winter due to persistent high-water pressure, which can incorporate the seasonal firn-aquifer water into the subglacial environment more rapidly than it would otherwise, thereby dampening the seasonal ice-velocity fluctuations (Poinar et al., 2019). In addition, firn aquifers have been predicted near the grounding lines of many ice shelves of the rapidly changing Antarctic Peninsula (AP), including the former Prince Gustav, Wilkins and Wordie ice shelves (van Wessem et al., 2021) and have been directly observed on the Wilkins ice shelf (Montgomery et al., 2020). Climate on the AP is similar to southeast Greenland, with high snow accumulation and high surface melt during the summer (Van Wessem et al., 2016; van Wessem et al., 2021) and even föhn-induced melt in the winter season (Munneke et al., 2014). With increasing precipitation rates (Thomas et al., 2008) and increasing atmospheric warming and surface melt (Bromwich et al., 2012), firn aquifers will be increasingly important to understand on the AP, as they may potentially accelerate the disintegration of ice shelves that buttress outlet glacier discharge to the oceans.

6 Conclusion

We assessed the extent of four firn aquifers in southeast Greenland through the last three decades using airborne ice-penetrating radar products. The accumulation radar (AR) data can detect the firn-aquifer water table and the radar depth-sounder (RDS) data can detect disappearance of the bed reflector due to the presence of the firn aquifer. We find that all four firn aquifers were initially identified along the flight line and/or show inland expansion during the observational period of 1993 to 2018. We find that this multidecadal firn-aquifer expansion is mainly driven by decreasing cold content and increasing surface melt, which has decreased the firn's capacity for refreezing since the late 1990s here. Specifically, recent warm, high-melt years such as 2007, 2010, and 2012 have decreased the firn's ability for refreezing adjacent to the upstream and at higher elevations to the edges of the firn-aquifer sites. Continued warming over the Greenland Ice Sheet (e.g., 2010 and 2012; Nghiem et al., 2012), increasing melt, and more frequent and intense high-melt years will likely contribute to a continued reduction in the firn's ability to refreeze meltwater through reducing the firn cold content and hindering top-down and lower-boundary refreezing of infiltrating meltwater, as well as introducing increased availability of meltwater. We may expect firn aquifers to continue to form and expand upstream in these regions of warming firn and to occupy greater areas of the Greenland Ice Sheet. Because of this, our understanding of how firn aquifers contribute to the Greenland Ice Sheet's mass balance, hydrology, and ice dynamics is vital. Future work should investigate broader-scale trends in aquifer behavior across Greenland and the Antarctic Peninsula; constrain in-situ meltwater flow and discharge measurements to refine the firn physics and to improve self-consistency of meltwater firn models; and downsize climate reanalysis data to finer grids to capture climate forcing on smaller scales at which firn-aquifer evolution occurs.

7 Code and Data Availability

Code for and output from the analysis is available at: `https://github.com/annikanhorlings/firn_aquifer_ice_penetrating_radar_analysis`. Outputs are also available from the authors without conditions. All ice-penetrating radar data used in this study are available from the CReSIS public FTP pages `ftp://data.cresis.ku.edu/data/accum/andhttps://data.cresis.ku.edu/data/rds/`, as well as the NSF Arctic Data Center at: `https://arcticdata.io/catalog/view/doi:10.18739/A2985M`. MARv3.5.2 climate model simulation outputs and metadata are available from the NSF Arctic Data Center at: `https://arcticdata.io/catalog/view/doi:10.18739/A21Z41T0T`. The DEM for Greenland is available on the NSIDC website at: `https://nsidc.org/data/NSIDC-0645/versions/1`.

8 Acknowledgements

ANH, KC, and CM designed the study. ANH interpreted the CReSIS data and MAR reanalysis data with input from KC. All authors contributed to writing the manuscript. We thank –, which funded this project. We are grateful to Sean O'Neil, who contributed to radar interpretation during the early part of this project. We also thank Nick Holschuh, Michelle Koutnik, and T.J. Fudge for comments on the manuscript draft.

References

Brangers, I., Lievens, H., Miège, C., Demuzere, M., Brucker, L., & De Lannoy, G. (2020). Sentinel-1 detects firn aquifers in the greenland ice sheet. *Geophysical Research Letters*, *47*(3), e2019GL085192.

Bromwich, D. H., Nicolas, J. P., Hines, K. M., Kay, J. E., Key, E. L., Lazzara, M. A., ... others (2012). Tropospheric clouds in antarctica. *Reviews of Geophysics*, *50*(1).

Christianson, K., Kohler, J., Alley, R. B., Nuth, C., & Van Pelt, W. J. (2015). Dynamic perennial firn aquifer on an arctic glacier. *Geophysical Research Letters*, *42*(5), 1418–1426.

Chu, W., Schroeder, D. M., & Siegfried, M. (2018). Retrieval of englacial firn aquifer thickness from ice-penetrating radar sounding in southeastern greenland. *Geophysical Research Letters*, *45*(21), 11–770.

Culberg, R., Schroeder, D. M., & Chu, W. (2021). Extreme melt season ice layers reduce firn permeability across greenland. *Nature communications*, *12*(1), 1–9.

Fettweis, X., & Rennermalm, A. (2020). Model simulations from modèle atmosphérique regionale (mar) over greenland, 1948-2016. *Nature Geoscience*.

Field, V, B., T, S., & Q, D. (2012). Managing the risks of extreme events and disasters to advance climate change adaptation: Special report of the intergovernmental panel on climate change.

Forster, R. R., Box, J. E., Van Den Broeke, M. R., Miège, C., Burgess, E. W., Van Angelen, J. H., ... others (2014). Extensive liquid meltwater storage in firn within the greenland ice sheet. *Nature Geoscience*, *7*(2), 95–98.

Fountain, A. G. (1989). The storage of water in, and hydraulic characteristics of, the firn of south cascade glacier, washington state, usa. *Annals of Glaciology*, *13*, 69–75.

Fountain, A. G., & Walder, J. S. (1998). Water flow through temperate glaciers. *Reviews of Geophysics*, *36*(3), 299–328.

Gascon, G., Sharp, M., Burgess, D., Bezeau, P., & Bush, A. B. (2013). Changes in accumulation-area firn stratigraphy and meltwater flow during a period of climate warming: Devon ice cap, nunavut, canada. *Journal of Geophysical Research: Earth Surface*, *118*(4), 2380–2391.

Humphrey, N. F., Harper, J. T., & Meierbachtol, T. W. (2021). Physical limits to meltwater penetration in firn. *Journal of Glaciology*, *67*(265), 952–960.

Jansson, P., Hock, R., & Schneider, T. (2003). The concept of glacier storage: a review. *Journal of Hydrology*, *282*(1-4), 116–129.

Killick, R., Fearnhead, P., & Eckley, I. A. (2012). Optimal detection of changepoints with a linear computational cost. *Journal of the American Statistical Association*, *107*(500), 1590–1598.

Koenig, L. S., Miège, C., Forster, R. R., & Brucker, L. (2014). Initial in situ measurements of perennial meltwater storage in the greenland firn aquifer. *Geophysical Research Letters*, *41*(1), 81–85.

Lavielle, M. (2005). Using penalized contrasts for the change-point problem. *Signal processing*, *85*(8), 1501–1510.

Legchenko, A., Miège, C., Koenig, L. S., Forster, R. R., Miller, O., Solomon, D. K., … Brucker, L. (2018). Estimating water volume stored in the south-eastern greenland firn aquifer using magnetic-resonance soundings. *Journal of Applied Geophysics*, *150*, 11–20.

Leuschen, C., Hale, R., Keshmiri, S., Yan, J., Rodriguez-Morales, F., Mahmood, A., & Gogineni, S. (2014). Uas-based radar sounding of the polar ice sheets. *IEEE Geoscience and Remote Sensing Magazine*, *2*(1), 8–17.

Lilien, D. A., Hills, B. H., Driscol, J., Jacobel, R., & Christianson, K. (2020). Impdar: an open-source impulse radar processor. *Annals of Glaciology*, *61*(81), 114–123.

Machguth, H., MacFerrin, M., van As, D., Box, J. E., Charalampidis, C., Colgan, W., … van de Wal, R. S. (2016). Greenland meltwater storage in firn limited by near-surface ice formation. *Nature Climate Change*, *6*(4), 390–393.

Miège, C., Forster, R. R., Brucker, L., Koenig, L. S., Solomon, D. K., Paden, J. D., … others (2016). Spatial extent and temporal variability of greenland firn aquifers detected by ground and airborne radars. *Journal of Geophysical Research: Earth Surface*, *121*(12), 2381–2398.

Miller, O., Solomon, D. K., Miège, C., Koenig, L., Forster, R., Schmerr, N., … others (2020). Hydrology of a perennial firn aquifer in southeast greenland: an overview driven by field data. *Water Resources Research*, *56*(8), e2019WR026348.

Montgomery, L., Miège, C., Miller, J., Scambos, T. A., Wallin, B., Miller, O., … Koenig, L. (2020). Hydrologic properties of a highly permeable firn aquifer in the wilkins ice shelf, antarctica. *Geophysical Research Letters*, *47*(22), e2020GL089552.

Mouginot, J., Rignot, E., Bjørk, A. A., Van den Broeke, M., Millan, R., Morlighem, M., … Wood, M. (2019). Forty-six years of greenland ice sheet mass balance from 1972 to 2018. *Proceedings of the national academy of sciences*, *116*(19), 9239–9244.

Munneke, P. K., Ligtenberg, S. R., Suder, E. A., & Van den Broeke, M. R. (2015). A model study of the response of dry and wet firn to climate change. *Annals of Glaciology*, *56*(70), 1–8.

Munneke, P. K., M. Ligtenberg, S., Van den Broeke, M., Van Angelen, J., & Forster, R. (2014). Explaining the presence of perennial liquid water bodies in the firn of the greenland ice sheet. *Geophysical Research Letters*, *41*(2), 476–483.

Nghiem, S., Hall, D., Mote, T., Tedesco, M., Albert, M., Keegan, K., … Neumann, G. (2012). The extreme melt across the greenland ice sheet in 2012. *Geophysical Research Letters*, *39*(20).

Ochwat, N. E., Marshall, S. J., Moorman, B. J., Criscitiello, A. S., & Copland, L. (2021). Evolution of the firn pack of kaskawulsh glacier, yukon: meltwater effects, densification, and the development of a perennial firn aquifer. *The Cryosphere*, *15*(4).

Oerter, H., & Rauert, W. (1982). Core drilling on vernagtferner (oetztal alps, austria) in 1979: tritium contents. *Zeitschrift für Gletscherkunde und Glazialgeologie*, *1*, 13–22.

Poinar, K., Dow, C. F., & Andrews, L. C. (2019). Long-term support of an active subglacial hydrologic system in southeast greenland by firn aquifers. *Geophysi-*

cal Research Letters, *46*(9), 4772–4781.

Poinar, K., Joughin, I., Lilien, D., Brucker, L., Kehrl, L., & Nowicki, S. (2017). Drainage of southeast greenland firn aquifer water through crevasses to the bed. *Frontiers in Earth Science*, *5*, 5.

Rodriguez-Morales, F., Gogineni, S., Leuschen, C. J., Paden, J. D., Li, J., Lewis, C. C., ... others (2013). Advanced multifrequency radar instrumentation for polar research. *IEEE Transactions on Geoscience and Remote Sensing*, *52*(5), 2824–2842.

Samimi, S., Marshall, S. J., Vandecrux, B., & MacFerrin, M. (2021). Time-domain reflectometry measurements and modeling of firn meltwater infiltration at dye-2, greenland. *Journal of Geophysical Research: Earth Surface*, *126*(10), e2021JF006295.

Schneider, T. (1999). Water movement in the firn of storglaciären, sweden. *Journal of Glaciology*, *45*(150), 286–294.

Shepherd, A., Ivins, E., Rignot, E., Smith, B., Van Den Broeke, M., Velicogna, I., ... others (2020). Mass balance of the greenland ice sheet from 1992 to 2018. *Nature*, *579*(7798), 233–239.

Thomas, E. R., Marshall, G. J., & McConnell, J. R. (2008). A doubling in snow accumulation in the western antarctic peninsula since 1850. *Geophysical research letters*, *35*(1).

Vandecrux, B., Mottram, R., Langen, P. L., Fausto, R. S., Olesen, M., Stevens, C. M., ... others (2020). The firn meltwater retention model intercomparison project (retmip): evaluation of nine firn models at four weather station sites on the greenland ice sheet. *The Cryosphere*, *14*(11), 3785–3810.

Van den Broeke, M. R., Enderlin, E. M., Howat, I. M., Kuipers Munneke, P., Noël, B. P., Van De Berg, W. J., ... Wouters, B. (2016). On the recent contribution of the greenland ice sheet to sea level change. *The Cryosphere*, *10*(5), 1933–1946.

Van Wessem, J., Ligtenberg, S., Reijmer, C., Van De Berg, W., Van Den Broeke, M., Barrand, N., ... others (2016). The modelled surface mass balance of the antarctic peninsula at 5.5 km horizontal resolution. *The Cryosphere*, *10*(1), 271–285.

van Wessem, J. M., Steger, C. R., Wever, N., & van den Broeke, M. R. (2021). An exploratory modelling study of perennial firn aquifers in the antarctic peninsula for the period 1979–2016. *The Cryosphere*, *15*(2), 695–714.

JGR: Earth Surface

Supporting Information for

Expansion of firn aquifers in southeast Greenland

Annika N. Horlings[1], Knut Christianson[1], Clément Miège[2]

[1]Department of Earth and Space Sciences, University of Washington, Seattle, WA, USA
[2]Department of Geography, University of Utah, Salt Lake City, Utah, USA

Contents of This File

S1. Introduction

This supporting information provides additional details on the radar methods and on the climate reanalysis time series analyzed for the four firn aquifer sites presented in the main manuscript. Sections S1-S4 provide more details on the radar methods and analysis of the firn aquifers via the CReSIS radar depth sounder data. Section S5 shows the repeat flight lines at each firn aquifer. Section S6 provides details on the change point calculation used on the climate reanalysis data. Section S7 shows analysis of parameters from MAR reanalysis data that are not shown in the main manuscript.

S2. Examples of RDS profiles with a contemporaneous AR profile

We first show two examples of contemporaneous CReSIS radar depth sounder (RDS) and accumulation radar (AR) profiles along a repeat flight line to illustrate the appearance of the firn aquifer in both data (Figures S1 and S2). The water table of the firn aquifer is the bright continuous reflector in the AR profiles which correlates with the disappearance of the bed reflector in the RDS profiles.

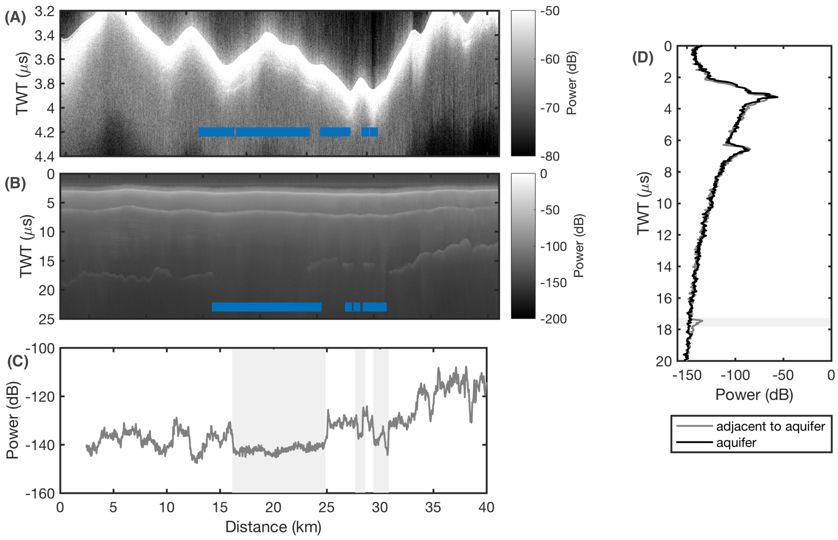

Figure S1. (A) AR data for Helheim 1 in 2013. (B) RDS data for Helheim 1 in 2013. (C) Power along the bed in the RDS data. (D) Traces selected within and outside of the aquifer region showing the lack of bed return in the aquifer in the RDS data. We choose to show this example to show the generally excellent agreement between the identification of the aquifer in the AR and RDS data.

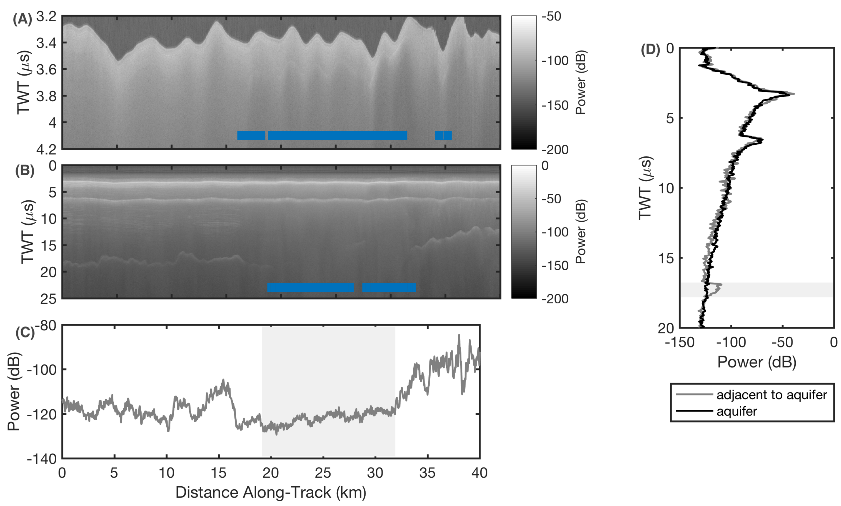

Figure S2. (A) AR data for Helheim 1 in 2012. (B) RDS data for Helheim 1 in 2012. (C) Power along the bed in the RDS data. (D) Traces selected within and outside of the aquifer region showing the lack of bed return in the aquifer in the RDS data. We choose this example to show that some slight disagreement between identification of the aquifer in the RDS and AR radar data is possible at the edges of the aquifer.

The power at the bed drops considerably (up to approximately 10 to 20 dB) at the main portion of the aquifer for a sustained distance (Figures S1C-D, S2C-D). There is not a distinct transition in and out of the main aquifer because, in reality, the distinction between the firn aquifer itself and surrounding dry firn is likely to be gradual and not spatially instantaneous (see section S4). Most disagreement between the different radar data occurs at the edges of the aquifer for this reason. We analyze individual traces (e.g., Figures S3-S6) to determine the location of the bed disappearance in the RDS profiles. While this disagreement is relatively low in all profiles, the aquifer identification within RDS data appears to underestimate the firn aquifer extent relative to the AR data when there is disagreement.

S3. Examples RDS profiles without a contemporaneous AR profile

Here, we show selected RDS profiles and highlight several repeat flight lines that do not have contemporaneous AR profiles (Figures S3-S6). We show two sets of profiles that illustrate the first appearance of the firn aquifers:(1) from H1, which distinctly shows a continuous bed reflector in 1993 and the appearance of the aquifer in 1998 (Figures S3-S4); and (2) from H4, which distinctly shows a continuous bed reflector in 1998 and shows the appearance of the firn aquifer in 2001 (Figures S5-S6).

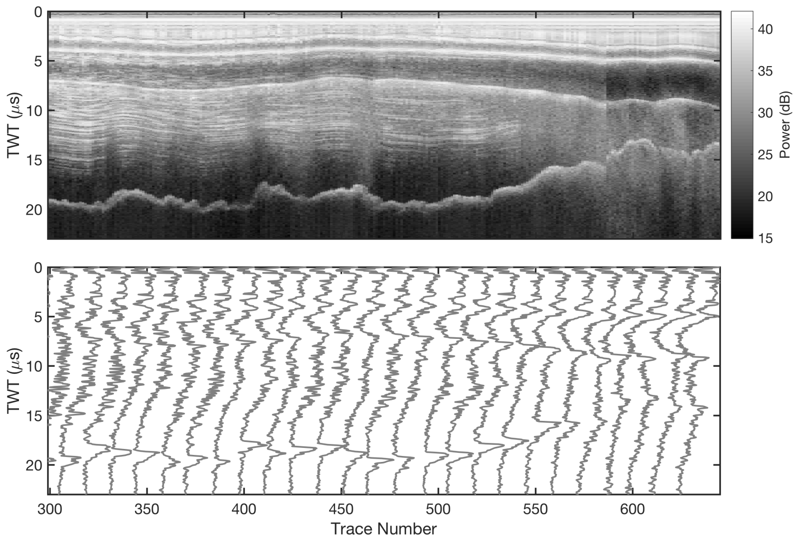

Figure S3. RDS profile at H1 in 1993. While the bed power can vary, the bed reflector is present through the entire profile, as distinctly shown by the single traces.

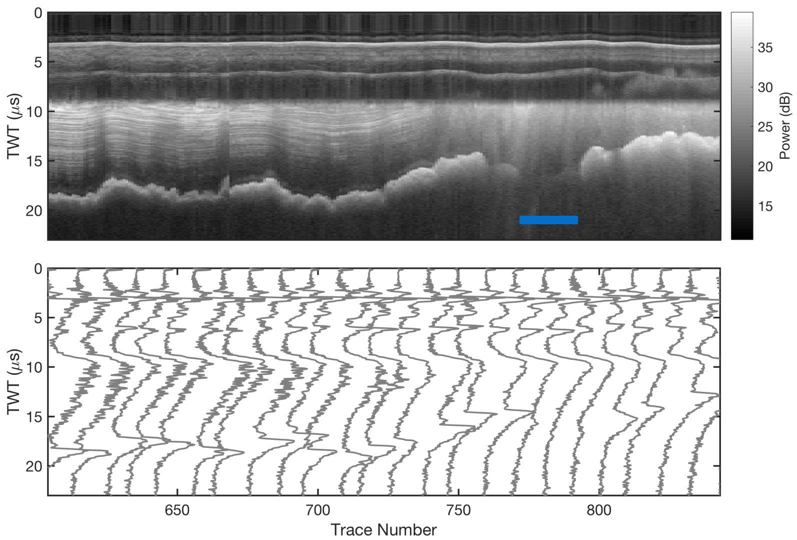

Figure S4. RDS profile at H1 in 1998. The bed reflector vanishes just after trace number 760 and corresponds to the aquifer pick shown.

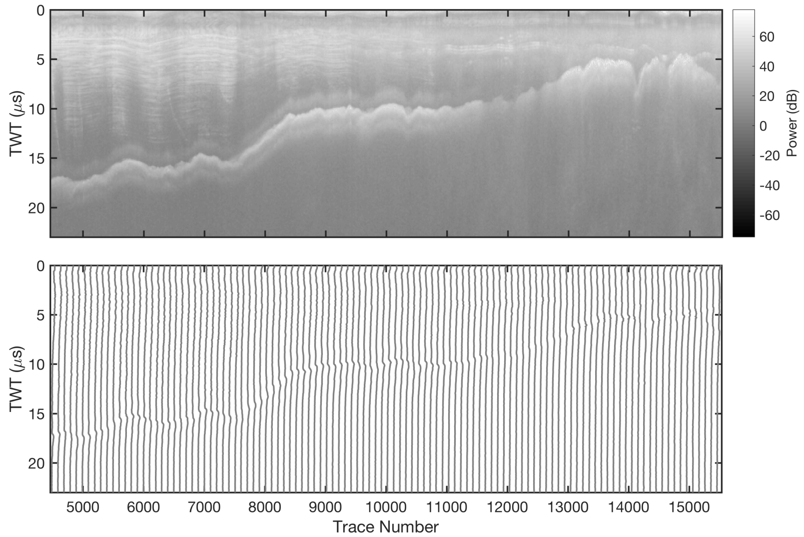

Figure S5. RDS profile at H4 in 1998. The single traces are plotted at small interval to show the features more clearly. While the bed power can vary, the bed reflector is present through the entire profile, as distinctly shown by the single traces.

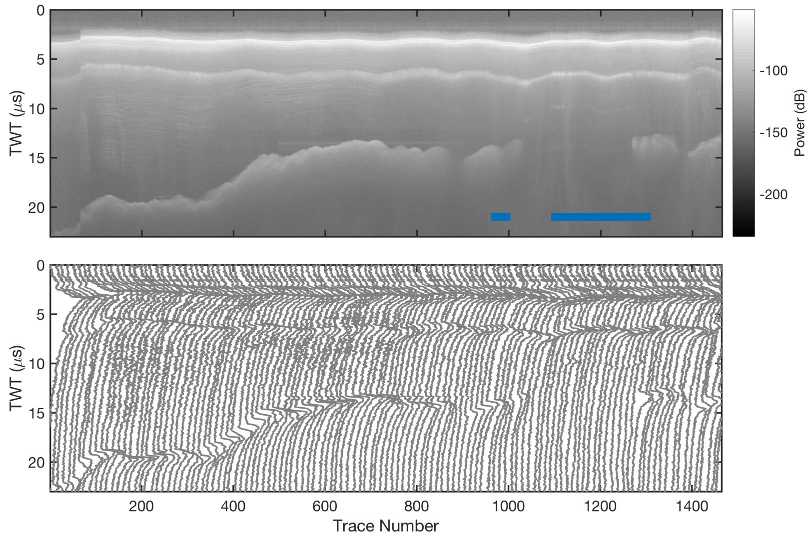

Figure S6. RDS profile at H4 in 2001. The bed reflector vanishes just after trace number 1000 and corresponds to the aquifer pick shown. ***[Fix misplaced detection in upstream part]

S4. Magnetic Resonance Data

Low water volumes from magnetic resonance soundings at H1 (Legchenko et al., 2018) correlate well with the bed reflector observed in the RDS data (Figure S8). Previous analysis also showed agreement between the water volumes and ground-penetrating radar data (Legchenko et al., 2018). Relatively low water volumes (<500 kg m^{-2}) from 25-27 km and 29-30 km along the flight line correlate with the reappearance of the bed reflector, whereas relatively high water volumes (>500 kg m^{-2}) correlate well with the aquifer.

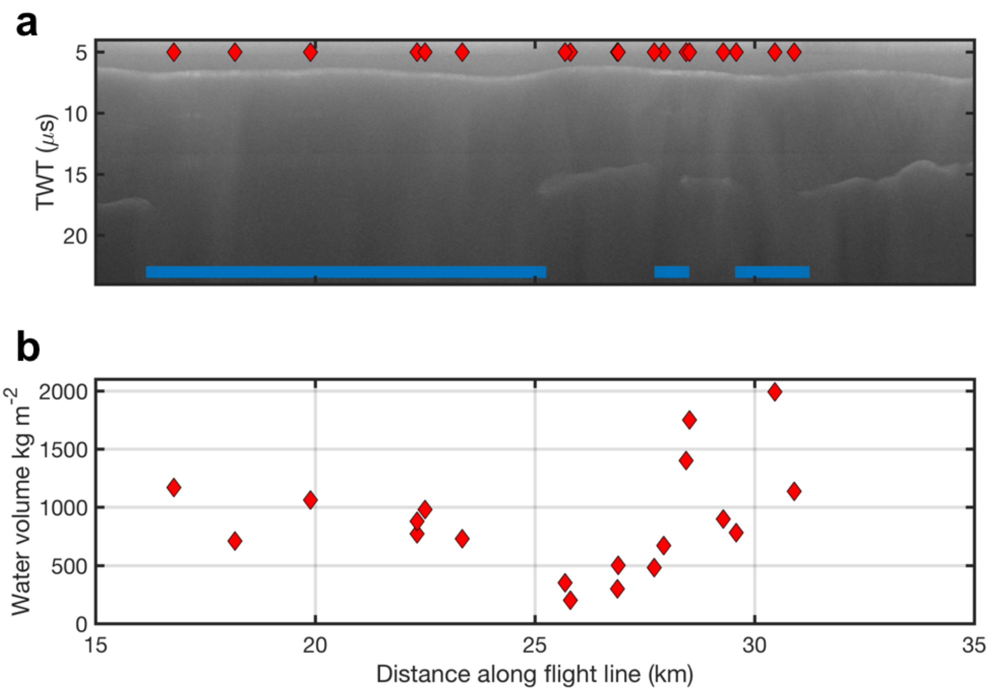

Figure S7. a) RDS profile at H1 in 2014 showing the extent of the firn aquifer (blue) and the location of the magnetic resonance measurements (red). b) Water volumes derived from the magnetic resonance measurements, taken in 2015 and 2016. Note that the nearest RDS profile in time is in 2014.

S5. Repeat Flight Lines at Each Aquifer Site

The repeat flight lines extend approximately over the same location each year, however, there are minor deviations. As such, we project the aquifer extent along the flight line to a common linear trajectory (Figure S8).

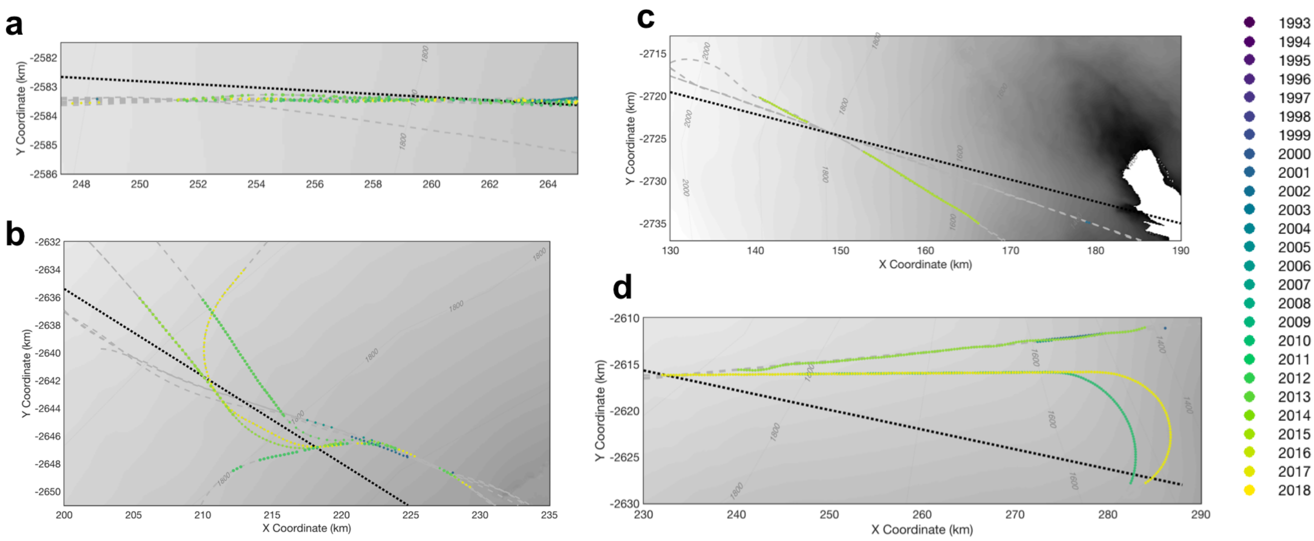

Figure S8. Repeat flight lines and aquifer detections for a) Helheim 1, b) Ikertivaq N1, c) Køge Bugt S1, and d) Helheim 4.

S6. Change Point Calculation of a Time Series

By definition, a change point is a time instant at which a defined statistical property, usually the mean, of a time series changes abruptly. We employ a parametric global method which selects a point to divide the time series into two sections, calculates an empiricial estimate of the mean for each section, computes the deviation of the time series from the empirical estimate of the mean, finds the total residual error, and varies the location of the point for which to divide the time series until the total residual error reaches a minimum. Given a time series x_1, x_2, ..., x_n, the method finds the point k such that the residual error r is the smallest:

$$r = \sum_{i=1}^{k-1} (x_i - \mu_{k-1})^2 + \sum_{i=k}^{N} (x_i - \mu_N)^2 - (k-1)V_{k-1} - (N-k+1)V_N. \tag{1}$$

where the mean for each section is defined as:

$$\mu_{k-1} = \frac{1}{k-1} \sum_{i=1}^{k-1} x_i \text{ and } \mu_N = \frac{1}{N-k+1} \sum_{i=k}^{N} x_i. \tag{2}$$

and the variance for each section is defined as:

$$V_{k-1} = \frac{1}{N-1} \sum_{i=1}^{k-1} x_i |A_i - \mu_{k-1}|^2 \text{ and } V_N = \frac{1}{N-1} \sum_{i=k}^{N} |A_i - \mu_N|^2. \tag{3}$$

S7. Additional Analysis of MAR Climate Reanalysis at Aquifer Sites

From the MAR Modèle Atmosphérique Régional MAR 3.5.2 (Fettweis and others, 2017) reanalysis, we analyze long-term trends in the climate variables noted in the main text. We take the average of these climate parameters for the closest MAR cells to the upstream edge of the aquifer sites because MAR's resolution is relatively coarse (20 km) for application to a single aquifer.

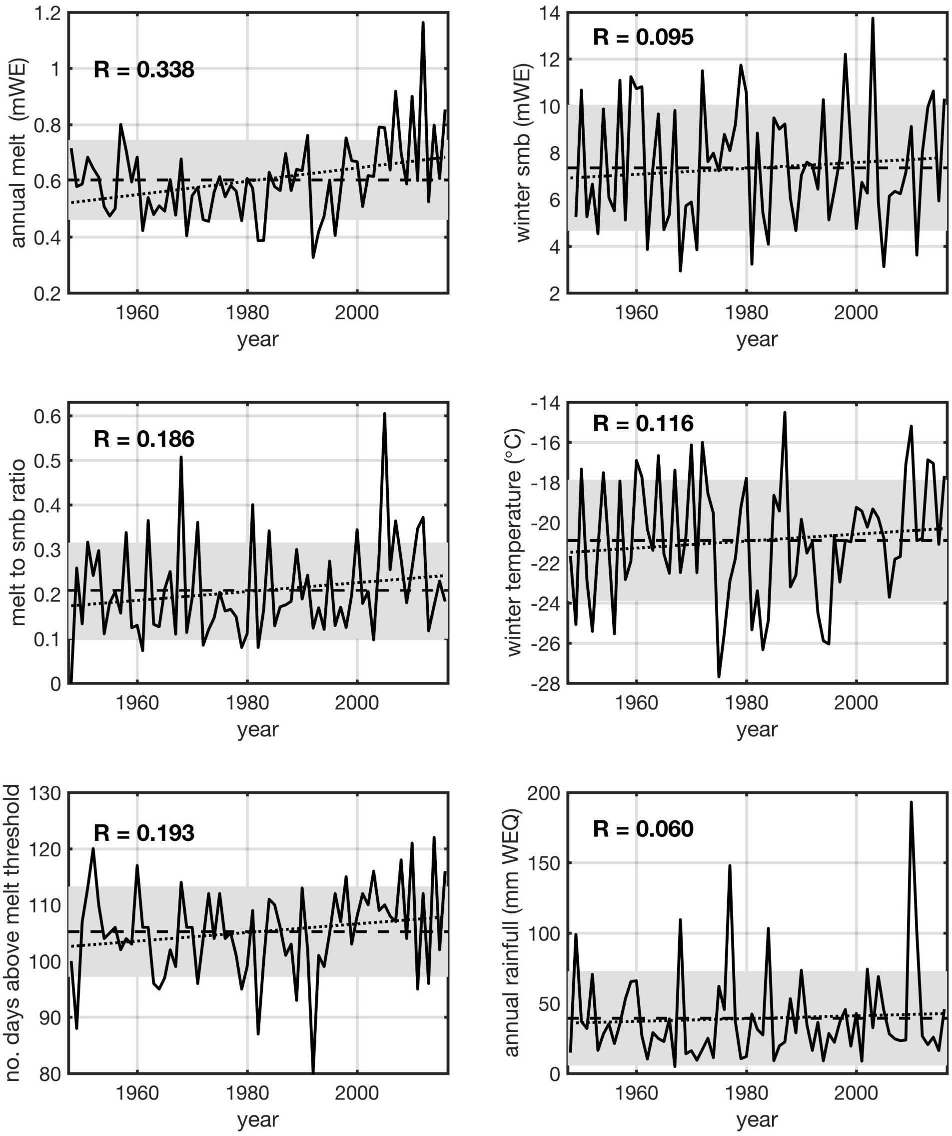

Figure S9. MAR output at the aquifer sites. (a) annual melt, (b) winter surface-mass-balance, (c) melt-to-surface-mass-balance ratio, (d) winter temperature, (e) number of days above the melt threshold, and (f) annual rainfall.

References

Brangers, I., Lievens, H., Miège, C., Demuzere, M., Brucker, L., & De Lannoy, G. (2020). Sentinel-1 detects firn aquifers in the greenland ice sheet. *Geophysical Research Letters*, *47*(3), e2019GL085192.

Bromwich, D. H., Nicolas, J. P., Hines, K. M., Kay, J. E., Key, E. L., Lazzara, M. A., … others (2012). Tropospheric clouds in antarctica. *Reviews of Geophysics*, *50*(1).

Christianson, K., Kohler, J., Alley, R. B., Nuth, C., & Van Pelt, W. J. (2015). Dynamic perennial firn aquifer on an arctic glacier. *Geophysical Research Letters*, *42*(5), 1418–1426.

Chu, W., Schroeder, D. M., & Siegfried, M. (2018). Retrieval of englacial firn aquifer thickness from ice-penetrating radar sounding in southeastern greenland. *Geophysical Research Letters*, *45*(21), 11–770.

Culberg, R., Schroeder, D. M., & Chu, W. (2021). Extreme melt season ice layers reduce firn permeability across greenland. *Nature communications*, *12*(1), 1–9.

Fettweis, X., & Rennermalm, A. (2020). Model simulations from modèle atmosphérique regionale (mar) over greenland, 1948-2016. *Nature Geoscience*.

Field, V, B., T, S., & Q, D. (2012). Managing the risks of extreme events and disasters to advance climate change adaptation: Special report of the intergovernmental panel on climate change.

Forster, R. R., Box, J. E., Van Den Broeke, M. R., Miège, C., Burgess, E. W., Van Angelen, J. H., … others (2014). Extensive liquid meltwater storage in firn within the greenland ice sheet. *Nature Geoscience*, *7*(2), 95–98.

Fountain, A. G. (1989). The storage of water in, and hydraulic characteristics of, the firn of south cascade glacier, washington state, usa. *Annals of Glaciology*, *13*, 69–75.

Fountain, A. G., & Walder, J. S. (1998). Water flow through temperate glaciers. *Reviews of Geophysics*, *36*(3), 299–328.

Gascon, G., Sharp, M., Burgess, D., Bezeau, P., & Bush, A. B. (2013). Changes in accumulation-area firn stratigraphy and meltwater flow during a period of climate warming: Devon ice cap, nunavut, canada. *Journal of Geophysical Research: Earth Surface*, *118*(4), 2380–2391.

Humphrey, N. F., Harper, J. T., & Meierbachtol, T. W. (2021). Physical limits to meltwater penetration in firn. *Journal of Glaciology*, *67*(265), 952–960.

Jansson, P., Hock, R., & Schneider, T. (2003). The concept of glacier storage: a review. *Journal of Hydrology*, *282*(1-4), 116–129.

Killick, R., Fearnhead, P., & Eckley, I. A. (2012). Optimal detection of changepoints with a linear computational cost. *Journal of the American Statistical Association*, *107*(500), 1590–1598.

Koenig, L. S., Miège, C., Forster, R. R., & Brucker, L. (2014). Initial in situ measurements of perennial meltwater storage in the greenland firn aquifer. *Geophysical Research Letters*, *41*(1), 81–85.

Lavielle, M. (2005). Using penalized contrasts for the change-point problem. *Signal processing*, *85*(8), 1501–1510.

Legchenko, A., Miège, C., Koenig, L. S., Forster, R. R., Miller, O., Solomon, D. K., … Brucker, L. (2018). Estimating water volume stored in the south-eastern greenland firn aquifer using magnetic-resonance soundings. *Journal of Applied Geophysics*, *150*, 11–20.

Leuschen, C., Hale, R., Keshmiri, S., Yan, J., Rodriguez-Morales, F., Mahmood, A., & Gogineni, S. (2014). Uas-based radar sounding of the polar ice sheets. *IEEE Geoscience and Remote Sensing Magazine*, *2*(1), 8–17.

Lilien, D. A., Hills, B. H., Driscol, J., Jacobel, R., & Christianson, K. (2020). Impdar: an open-source impulse radar processor. *Annals of Glaciology*, *61*(81), 114–123.

Machguth, H., MacFerrin, M., van As, D., Box, J. E., Charalampidis, C., Colgan, W., ... van de Wal, R. S. (2016). Greenland meltwater storage in firn limited by near-surface ice formation. *Nature Climate Change*, *6*(4), 390–393.

Miège, C., Forster, R. R., Brucker, L., Koenig, L. S., Solomon, D. K., Paden, J. D., ... others (2016). Spatial extent and temporal variability of greenland firn aquifers detected by ground and airborne radars. *Journal of Geophysical Research: Earth Surface*, *121*(12), 2381–2398.

Miller, O., Solomon, D. K., Miège, C., Koenig, L., Forster, R., Schmerr, N., ... others (2020). Hydrology of a perennial firn aquifer in southeast greenland: an overview driven by field data. *Water Resources Research*, *56*(8), e2019WR026348.

Montgomery, L., Miège, C., Miller, J., Scambos, T. A., Wallin, B., Miller, O., ... Koenig, L. (2020). Hydrologic properties of a highly permeable firn aquifer in the wilkins ice shelf, antarctica. *Geophysical Research Letters*, *47*(22), e2020GL089552.

Mouginot, J., Rignot, E., Bjørk, A. A., Van den Broeke, M., Millan, R., Morlighem, M., ... Wood, M. (2019). Forty-six years of greenland ice sheet mass balance from 1972 to 2018. *Proceedings of the national academy of sciences*, *116*(19), 9239–9244.

Munneke, P. K., Ligtenberg, S. R., Suder, E. A., & Van den Broeke, M. R. (2015). A model study of the response of dry and wet firn to climate change. *Annals of Glaciology*, *56*(70), 1–8.

Munneke, P. K., M. Ligtenberg, S., Van den Broeke, M., Van Angelen, J., & Forster, R. (2014). Explaining the presence of perennial liquid water bodies in the firn of the greenland ice sheet. *Geophysical Research Letters*, *41*(2), 476–483.

Nghiem, S., Hall, D., Mote, T., Tedesco, M., Albert, M., Keegan, K., … Neumann, G. (2012). The extreme melt across the greenland ice sheet in 2012. *Geophysical Research Letters*, *39*(20).

Ochwat, N. E., Marshall, S. J., Moorman, B. J., Criscitiello, A. S., & Copland, L. (2021). Evolution of the firn pack of kaskawulsh glacier, yukon: meltwater effects, densification, and the development of a perennial firn aquifer. *The Cryosphere*, *15*(4).

Oerter, H., & Rauert, W. (1982). Core drilling on vernagtferner (oetztal alps, austria) in 1979: tritium contents. *Zeitschrift für Gletscherkunde und Glazialgeologie*, *1*, 13–22.

Poinar, K., Dow, C. F., & Andrews, L. C. (2019). Long-term support of an active subglacial hydrologic system in southeast greenland by firn aquifers. *Geophysical Research Letters*, *46*(9), 4772–4781.

Poinar, K., Joughin, I., Lilien, D., Brucker, L., Kehrl, L., & Nowicki, S. (2017). Drainage of southeast greenland firn aquifer water through crevasses to the bed. *Frontiers in Earth Science*, *5*, 5.

Rodriguez-Morales, F., Gogineni, S., Leuschen, C. J., Paden, J. D., Li, J., Lewis, C. C., … others (2013). Advanced multifrequency radar instrumentation for polar research. *IEEE Transactions on Geoscience and Remote Sensing*, *52*(5), 2824–2842.

Samimi, S., Marshall, S. J., Vandecrux, B., & MacFerrin, M. (2021). Time-domain reflectometry measurements and modeling of firn meltwater infiltration at dye-2, greenland. *Journal of Geophysical Research: Earth Surface*, *126*(10), e2021JF006295.

Schneider, T. (1999). Water movement in the firn of storglaciären, sweden. *Journal of Glaciology*, *45*(150), 286–294.

Shepherd, A., Ivins, E., Rignot, E., Smith, B., Van Den Broeke, M., Velicogna, I., … others

(2020). Mass balance of the greenland ice sheet from 1992 to 2018. *Nature*, *579*(7798), 233–239.

Thomas, E. R., Marshall, G. J., & McConnell, J. R. (2008). A doubling in snow accumulation in the western antarctic peninsula since 1850. *Geophysical research letters*, *35*(1).

Vandecrux, B., Mottram, R., Langen, P. L., Fausto, R. S., Olesen, M., Stevens, C. M., ... others (2020). The firn meltwater retention model intercomparison project (retmip): evaluation of nine firn models at four weather station sites on the greenland ice sheet. *The Cryosphere*, *14*(11), 3785–3810.

Van den Broeke, M. R., Enderlin, E. M., Howat, I. M., Kuipers Munneke, P., Noël, B. P., Van De Berg, W. J., ... Wouters, B. (2016). On the recent contribution of the greenland ice sheet to sea level change. *The Cryosphere*, *10*(5), 1933–1946.

Van Wessem, J., Ligtenberg, S., Reijmer, C., Van De Berg, W., Van Den Broeke, M., Barrand, N., ... others (2016). The modelled surface mass balance of the antarctic peninsula at 5.5 km horizontal resolution. *The Cryosphere*, *10*(1), 271–285.

van Wessem, J. M., Steger, C. R., Wever, N., & van den Broeke, M. R. (2021). An exploratory modelling study of perennial firn aquifers in the antarctic peninsula for the period 1979–2016. *The Cryosphere*, *15*(2), 695–714.